Quantum Inf Process (2013) 12:1835–1850
DOI 10.1007/s11128-012-0496-2

On a three-parameter quantum *battle of the sexes* cellular automaton

Ramón Alonso-Sanz

Received: 22 June 2012 / Accepted: 6 October 2012 / Published online: 19 October 2012

Abstract The dynamics of a spatial quantum formulation of the iterated *battle of the sexes* game is studied in this work. The game is played in the cellular automata manner, i.e., with local and synchronous interaction. The effect of spatial structure is assessed when allowing the players to adopt quantum strategies that are no restricted to any particular subset of the possible strategies.

Keywords Quantum · Games · Spatial · Cellular automata

1 Introduction: the non-quantum context

The so called *battle of the sexes* (BOS) is a simple example of a two-person (♀ and ♂) asymmetric game, i.e., a game whose payoff matrices are not coincident after transposition [7,21]. Thus, for example: $\mathbf{P}_{♂} = \begin{pmatrix} R & 0 \\ 0 & r \end{pmatrix}$, and $\mathbf{P}_{♀} = \begin{pmatrix} r & 0 \\ 0 & R \end{pmatrix}$. The rewards $R > r > 0$ quantify the preferences in a conventional couple fitting the traditional stereotypes: the male prefers to attend a *F*ootball match, whereas the female prefers to attend a *B*allet performance. Both players decide hoping to *coordinate* their choices, but the *conflict* component is also present because their preferred activities differ. The BOS game epitomizes the class of *bimatrix* games, which have been used to model asymmetric (albeit not unfair) contests both in biology [17] and in economics [16].

Using uncorrelated probabilistic strategies $\mathbf{x} = (x, 1-x)'$ and $\mathbf{y} = (y, 1-y)'$, the expected payoffs (p) in the BOS game are:

R. Alonso-Sanz (✉)
Universidad Politecnica de Madrid, ETSI Agrónomos (Estadística, GSC) C. Universitaria, 28040 Madrid, Spain
e-mail: ramon.alonso@upm.es

$$p_{\male}(x;\, y) = \mathbf{x}'\mathbf{P}_{\male}\mathbf{y}, \quad p_{\female}(y;\, x) = \mathbf{x}'\mathbf{P}_{\female}\mathbf{y}. \tag{1}$$

The pair of strategies $(\mathbf{x}, \mathbf{y})$ are in Nash equilibrium if $\mathbf{x}$ is a best response to $\mathbf{y}$ and $\mathbf{y}$ is a best response to $\mathbf{x}$. There are three pairs of strategies in Nash equilibrium in the BOS game [1].

Both players get the same payoff if $y = 1-x$, with a maximum $p^+ = (R+r)/4$ for $x = y = 1/2$. Thus, payoff region $(p_{\female}, p_{\male})$ is closed by the parabola passing through (R, r), (r, R), and (p^+, p^+).

In a broader game scenario, a probability distribution $\mathbf{A} = (a_{ij})$ assigns probability to every combination of player choices, so $\mathbf{A} = \begin{pmatrix} a_{11} & a_{12} \\ a_{21} & a_{22} \end{pmatrix}$ in 2×2 games [21]. Thus, the expected payoffs in the BOS are: $\begin{matrix} p_{\male} = a_{11}R + a_{22}r \\ p_{\female} = a_{11}r + a_{22}R \end{matrix}$, and the payoff region is now limited to the triangle with vertices $(0, 0)$, (R, r) and (r, R). In this scenario, both players get the same payoff if $a_{11} = a_{22} = a$, with $p^= = a(R + r)$. So that if $a > 1/4$ the players get equalitarian payoffs that are not accessible in the uncorrelated strategies scenario. The maximum equalitarian payoff $p^= = (R + r)/2$ is reached with $a = 1/2$.

2 Quantum games

In the quantization scheme introduced by Eisert et al. [11], the classical strategies F and B are assigned two basic vectors $|0\rangle$ and $|1\rangle$ respectively, in a Hilbert space of a two level system. The state of the game is a vector in the tensor product space spanned by the basis vectors $|00\rangle$, $|01\rangle$, $|10\rangle$, $|11\rangle$, where the first entry in the ket refers to the male player (termed A in the general scheme) and the second entry refers to the female (termed B in the general scheme) player.

The quantum game protocol starts with an initial entangled state $|\psi_i\rangle = \hat{J}|00\rangle$, where $\hat{J}$ is a symmetric unitary operator that *entangles* the players qubits and that is known to both players. To ensure that the classical game is a subset of its quantum version, it is necessary that $\hat{J} = exp(i\frac{\gamma}{2}\hat{D}^{\otimes 2})$, where $\gamma \in [0, \pi/2]$. With classical strategies, $\hat{D} = \begin{pmatrix} 0 & 1 \\ -1 & 0 \end{pmatrix}$, $\hat{I} = \begin{pmatrix} 1 & 0 \\ 0 & 1 \end{pmatrix}$.

The players perform their quantum strategies as local unitary operators $(\hat{U})$ in SU(2), $\hat{U}_A$ and $\hat{U}_B$. After the application of these strategies, that the players chose independently, the state of the game evolves to $|\psi_{f_o}\rangle = (\hat{U}_A \otimes \hat{U}_B)\hat{J}|00\rangle$. Prior to measurement, the $\hat{J}^\dagger$ gate is applied and the state of the game becomes:

$$|\psi_f\rangle = \hat{J}^\dagger(\hat{U}_A \otimes \hat{U}_B)\hat{J}|00\rangle \equiv (\psi_1\psi_2\psi_3\psi_4)' \tag{2}$$

This follows a pair of Stern-Gerlach type detectors for measurement. As a result, $\mathbf{A} = \begin{pmatrix} |\psi_1|^2 & |\psi_2|^2 \\ |\psi_3|^2 & |\psi_4|^2 \end{pmatrix}$. Consequently, the expected payoffs become:

$$p\begin{Bmatrix} A \\ B \end{Bmatrix} = \begin{Bmatrix} R \\ r \end{Bmatrix} |\psi_1|^2 + \begin{Bmatrix} r \\ R \end{Bmatrix} |\psi_4|^2 \tag{3}$$

With maximal entangling ($\gamma = \pi/2$): $\hat{J} = \frac{1}{\sqrt{2}}(\hat{I}^{\otimes 2} + i\hat{D}^{\otimes 2})$. Thus, $\hat{J}|00\rangle = \frac{1}{\sqrt{2}}\begin{pmatrix} 1 & 0 & 0 & i \\ 0 & 1 & -i & 0 \\ 0 & -i & 1 & 0 \\ i & 0 & 0 & 1 \end{pmatrix}\begin{pmatrix} 1 \\ 0 \\ 0 \\ 0 \end{pmatrix} = \frac{1}{\sqrt{2}}\begin{pmatrix} 1 \\ 0 \\ 0 \\ i \end{pmatrix}$, and $\hat{J}^\dagger = \frac{1}{\sqrt{2}}\begin{pmatrix} 1 & 0 & 0 & -i \\ 0 & 1 & i & 0 \\ 0 & i & 1 & 0 \\ -i & 0 & 0 & 1 \end{pmatrix}$.

We will give here consideration to the full space of SU(2) strategies, i.e., the three-parameter strategies [6]:

$$\hat{U}(\theta, \alpha, \beta) = \begin{pmatrix} e^{i\alpha}\cos(\theta/2) & e^{i\beta}\sin(\theta/2) \\ -e^{-i\beta}\sin(\theta/2) & e^{-i\alpha}\cos(\theta/2) \end{pmatrix}, \begin{matrix} \theta \in [0, \pi] \\ \alpha, \beta \in [0, \pi/2] \end{matrix}. \tag{4}$$

By contrast, in the seminal article by Eisert et al. [11] and in our study [1], the two-parameter (2P) subset with no β [or $\beta = 0$ in (4)] is considered.

Nash Equilibrium is achieved in two ways in the two-parameter model [14]. But no pair of strategies in Nash equilibrium exists in the three-parameter model with maximum entanglement [6].

If $\alpha_A = \alpha_B = \beta_A = \beta_B = 0$, it is: $\mathbf{A} = \begin{pmatrix} \cos^2\omega_A \\ \sin^2\omega_A \end{pmatrix}\begin{pmatrix} \cos^2\omega_B & \sin^2\omega_B \end{pmatrix}$, noting $\omega \equiv \theta/2$. Thus, the joint probabilities factorize as in the *classical* game employing independent strategies (1) with $x = \cos^2\theta_A$, $y = \cos^2\theta_B$. So to say, the θ parameters are the *classical* ones.

In contrast, if $\theta_A = \theta_B = 0$, it is: $\mathbf{A} = \begin{pmatrix} \cos^2(\alpha_A + \alpha_B) & 0 \\ 0 & \sin^2(\alpha_A + \alpha_B) \end{pmatrix}$, a no factorizable joint probability distribution. In the particular case $\alpha_A + \alpha_B = \pi/4$, it is $a_{11} = a_{22} = 1/2$. It is noticeable that the β parameter is absent in the $\theta = 0$ scenario, i.e., the roles of the α and β parameters are not interchangeable.

3 The spatialized Q-BOS

Spatialized quantum games are fairly unexplored. Even in its simplest form, i.e., in the cellular automaton (CA)[1]-manner described below. The reader unfamiliar with the CA literature should not confuse the quantum-game CA approach proposed here with general quantum CA models [23].

In the spatial version of the BOS we deal with, each player occupies a site (i, j) in a two-dimensional $N \times N$ lattice. We will consider that *males* and *females* alternate in the site occupation in a chessboard form. Thus, every player is surrounded by four partners (♀-♂, ♂-♀), and four mates (♀-♀, ♂-♂).

[1] Cellular automata are spatially extended dynamical systems that are discrete in all their constitutional components: space, time and state-variable. Uniform, local and synchronous interactions, as assumed here, are landmark features of CA [22].

In a cellular automata-like implementation, in each generation (T) every player plays with his four adjacent partners, so that the payoff $p_{i,j}^{(T)}$ of a given individual is the sum over these four interactions. In the next generation, every player will adopt the parameter choice $(\alpha_{i,j}^{(T)}, \theta_{i,j}^{(T)}, \beta_{i,j}^{(T)})$ of his nearest-neighbor mate (including himself) that received the highest payoff. In case of a tie, i.e., several mate neighbors with the same maximum payoff, the average of the (θ, α, β) parameter values corresponding to the best mate neighbors will be adopted.

To make sure that the players in the borders are in the regular conditions regarding mate and partner neighborhood, periodic boundary conditions and even side size lattice are needed. All the simulations in this work are run in a $N = 200$ lattice.

Figure 1 deals with four simulations starting at random with respect to the parameter values in a quantum ($R = 5$, $r = 1$)-BOS cellular automaton. The far left panel of the figure shows the evolution up to $T = 200$ of the mean values across the lattice of θ, α, and β, as well of the actual mean payoffs. Figure 1 shows also snapshots of the parameter and payoff patterns at $T = 200$.

As a result of the random assignment of the parameter values it is initially: $\overline{\theta}_{\male} \simeq \overline{\theta}_{\female} \simeq \pi/2 = 1.57$, and $\overline{\alpha}_{\male} \simeq \overline{\alpha}_{\female} \simeq \overline{\beta}_{\male} \simeq \overline{\beta}_{\female} \simeq \pi/4 = 0.78$. Consequently, the mean payoffs are initially $\overline{p}_{\male} \simeq \overline{p}_{\female} \simeq 1.5$, very close to the mean payoffs $p_{\male} = p_{\female} = 1.5$ achieved in a two-person game with equal middle-level election of the parameters by both players, i.e. $\theta_A = \theta_B = \pi/2, \alpha_A = \alpha_B = \beta_A = \beta_B = \pi/4$, in which case:

$$
\begin{aligned}
\hat{U}_A &= \hat{U}_B = \frac{1}{\sqrt{2}}\frac{1}{\sqrt{2}}\begin{pmatrix} 1+i & 1+i \\ -(1-i) & 1-i \end{pmatrix} \\
(\hat{U}_A \otimes \hat{U}_B) &= \frac{1}{4}\begin{pmatrix} (1+i)^2 & (1+i)^2 & (1+i)^2 & (1+i)^2 \\ -(1+i)(1-i) & (1+i)(1-i) & -(1+i)(1-i) & (1+i)(1-i) \\ -(1-i)(1+i) & -(1-i)(1+i) & (1-i)(1+i) & (1-i)(1+i) \\ (1-i)^2 & -(1-i)(1-i) & -(1-i)^2 & (1-i)^2 \end{pmatrix} \\
&= \frac{1}{2}\begin{pmatrix} i & i & i & i \\ -1 & 1 & -1 & 1 \\ -1 & -1 & 1 & 1 \\ -i & i & i & -i \end{pmatrix} \\
|\psi_f\rangle &= \hat{J}^\dagger(\hat{U}_A \otimes \hat{U}_B)\hat{J}|00\rangle = \hat{J}^\dagger \frac{1}{2\sqrt{2}}\begin{pmatrix} i-1 \\ i-1 \\ i-1 \\ 1-i \end{pmatrix} = \frac{1}{4}\begin{pmatrix} -2i \\ -2 \\ -2 \\ -2i \end{pmatrix},
\end{aligned}
$$

so that the probability distribution matrix is: $\mathbf{A} = \begin{pmatrix} 1/4 & 1/4 \\ 1/4 & 1/4 \end{pmatrix} \Rightarrow p_{\female} = p_{\male} = \frac{R+r}{4}$, the arithmetic mean of the payoff values, i.e., $p^+ = (R+r)/4 = 1.5$.

Thus, in the three-parameter model, the Eisert et al. protocol is free of the bias towards the female player present in the two-parameter scheme, in which the equal

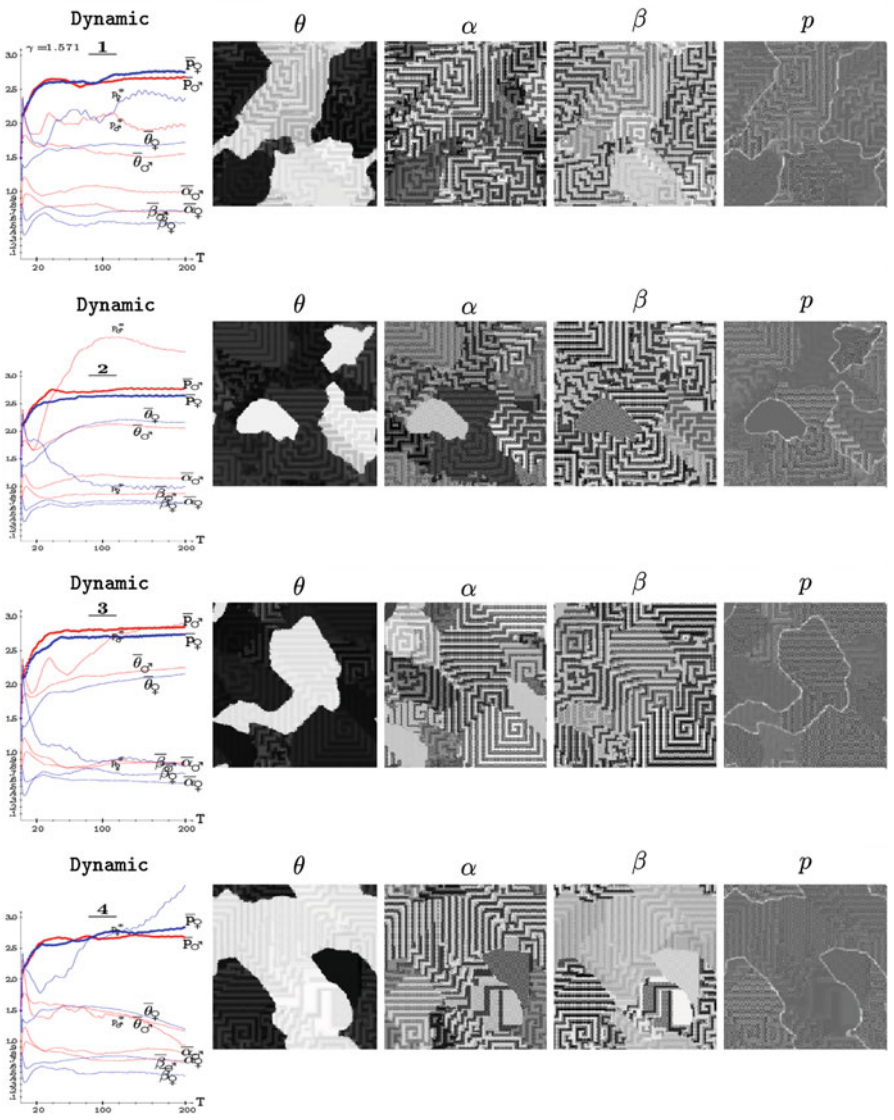

Fig. 1 Four simulations of a three-parameter quantum (5,1)-BOS cellular automaton. *Far left* evolving mean parameters and payoffs. *Center* parameter patterns at $T = 200$. *Far right* payoff patterns at $T = 200$. Increasing gray levels indicate increasing parameter values

middle-level election of parameters, i.e., $\theta_A = \theta_B = \pi/2, \alpha_A = \alpha_B = \pi/4$, leads to $a_{22} = 1$[2] $\Rightarrow p_{\male} = r < p_{\female} = R$.

2

$$\hat{U}_A = \hat{U}_B = \begin{pmatrix} \frac{1}{\sqrt{2}}(1+i)\frac{1}{\sqrt{2}} & \frac{1}{\sqrt{2}} \\ -\frac{1}{\sqrt{2}} & \frac{1}{\sqrt{2}}(1-i)\frac{1}{\sqrt{2}} \end{pmatrix} = \frac{1}{2}\begin{pmatrix} 1+i & \sqrt{2} \\ -\sqrt{2} & 1-i \end{pmatrix}$$

Accordingly with the absence of bias favouring any of the types of players, in the three-parameter simulations of Fig. 1 both mean payoffs evolve in a fairly parallel way, so that in two of the simulations the male mean payoff is slightly over the mean female payoff, and in the two other simulations the relation is the reverse. In any of the simulations, the spatial ordered structure induces a kind of self-organization effect, which allows to achieve fairly soon pairs of mean payoffs that are accessible only with correlated strategies in the two-person game. Recall that the maximum equalitarian payoff in the uncorrelated context is $p^+ = (\mathrm{R} + \mathrm{r})/4 = 1.5$, whereas the payoffs in the simulations of Fig. 1 reach values over 2.5, not far from the maximum feasible equalitarian payoff $p^= = (R + r)/2 = 3.0$.

The mean α and β parameter values of both kinds of players remain fairly stable in the simulations in Fig. 1, not far from the initial $\pi/4 = 0.78$ mean value. In contrast, the θ parameters exhibit a greater diversity in their behaviour. Thus, in simulations -1- and -2- the θ parameters tend to stabilization fairly soon, whereas in simulations -3- and -4- increasing and decreasing tendencies appear. In the simulation -3- the θ parameters still grow beyond $T = 200$, and nearly stabilize at $T = 900$, reaching at $T = 1000 : \theta_{♀} = 2.50, \theta_{♂} = 2.39$. In simulation -4-, the θ parameters decrease very slowly, reaching at $T = 1000$: $\theta_{♀} = 0.33, \theta_{♂} = 0.36$.

The curves labelled p^* in the far left panel of Fig. 1 show the *theoretical* (or *mean-field*) payoffs of both players, i.e., the payoffs achieved for both kinds of players in a single hypothetical two-person game with players adopting the mean parameters appearing in the spatial dynamic simulation. Namely,

$$U^*_{♂} = \begin{pmatrix} e^{i\overline{\alpha}_{♂}} \cos\overline{\omega}_{♂} & e^{i\overline{\beta}_{♂}} \sin\overline{\omega}_{♂} \\ -e^{-i\overline{\beta}_{♂}} \sin\overline{\omega}_{♂} & e^{-i\overline{\alpha}_{♂}} \cos\overline{\omega}_{♂} \end{pmatrix}, \; U^*_{♀} = \begin{pmatrix} e^{i\overline{\alpha}_{♀}} \cos\overline{\omega}_{♀} & e^{i\overline{\beta}_{♀}} \sin\overline{\omega}_{♀} \\ -e^{-i\overline{\beta}_{♀}} \sin\overline{\omega}_{♀} & e^{-i\overline{\alpha}_{♀}} \cos\overline{\omega}_{♀} \end{pmatrix}.$$

The p^* values shown in Fig. 1 appear to poorly reflect the actual mean payoffs of both kinds of players. The spatial structure marks the difference, so that often they are not very much indicative of the actual spatial mean payoffs The exception to this seems to be the case of simulation -1- in Fig. 1, in which both theoretical payoffs evolve qualitatively as the actual payoffs do. In the remaining three simulations of Fig. 1, the $p^*_{♀}$ and $p^*_{♂}$ values notably diverge, unlike the actual $\overline{p}_{♀}$ and $\overline{p}_{♂}$. Particularly remarkable following this behaviour is the simulation -4-, where the theoretical payoffs drift to near 5 and to near 1, whereas the actual mean payoffs remain fairly stable.

Foonote 2 continued

$$(\hat{U}_A \otimes \hat{U}_B) = \frac{1}{4} \begin{pmatrix} 2i & (1+i)\sqrt{2} & \sqrt{2}(1+i) & 2 \\ -(1+i)\sqrt{2} & 2 & -2 & -\sqrt{2}(1-i) \\ -\sqrt{2}(1+i) & -2 & 2 & (1-i)\sqrt{2} \\ 2 & -\sqrt{2}(1-i) & -(1-i)\sqrt{2} & -2i \end{pmatrix}$$

$$|\psi_f\rangle = \hat{J}^\dagger(\hat{U}_A \otimes \hat{U}_B)\hat{J}|00\rangle = \hat{J}^\dagger \frac{1}{4\sqrt{2}} \begin{pmatrix} 4i \\ -2\sqrt{2} \\ -2i\sqrt{2} \\ 4 \end{pmatrix} = \frac{1}{8} \begin{pmatrix} 0 \\ 0 \\ 0 \\ 8 \end{pmatrix}$$

In the -4- simulation up to $T = 1000$, it is: $p^*_{\varphi} = 4.75$, $p^*_{\sigma} = 1.12$, $\overline{p}_{\varphi} = 2.89$, $\overline{p}_{\sigma} = 2.78$.

Figure 2 shows early patterns in the simulation -3- of Fig. 1. The initial patterns show a sort of fine-grained *patchwork* aspect, but by $T = 40$ a maze aspect commences to emerge in the α and β patterns, whereas nucleation seems to predominate in the θ and payoff patterns. These tendencies are reinforced when progressing in the dynamics, so that in the four simulations shown in Fig. 1, at $T = 200$ maze-like structures predominate in the α and β parameter patterns, whereas coordination clusters are predominant in what respect to the θ parameter, much as happens in the classical spatialized BOS [2–4]. In any case, both maze-like structures and coordination clusters may be appreciated at some extent in every parameter pattern, and in the payoffs patterns, where the interfaces of disagreement in the parameters (leading to low $|\psi_1|^2$ and $|\psi_4|^2$) are tenuously visible.

It is remarkable that although the initial parameter pattern configuration plays a role in the details of the evolving dynamics, the main features of the dynamics are common to any simulation.

4 Unfair contests

Let us assume the unfair situation: B is restricted to classical strategies $\tilde{U}(\theta_B, 0, 0)$, whereas A may use quantum $\hat{U}(\theta_A, \alpha_A, \beta_A)$ ones.

Figure 3 shows four simulations of a quantum (5,1)-BOS cellular automaton, where the female players are restricted to classical strategies, i.e., $\alpha_{\varphi} = \beta_{\varphi} = 0$. As a result of the unfair scenario, the left panel of the figure shows how male players rapidly get mean payoffs near the maximum $R = 5$, whereas the female are induced to get mean values very close to $r = 1$. It is very remarkable the high coincidence of the evolving θ values of both kinds of players all along the evolution of the four simulations in Fig. 3. This corresponds with the very well defined areas of coordinated players (well defined black or blank regions) in the θ-patterns shown at $T = 200$ in the figure. Further dynamics is qualitatively different in the four simulations. In simulation -1- the parameter levels reached at $T = 200(\overline{\theta}_{\sigma} = 1.93 \simeq \overline{\theta}_{\sigma} = 1.90, \overline{\alpha}_{\sigma} = 0.89, \overline{\beta}_{\sigma} = 1.20)$ are almost stable, and consequently the patterns shown in the figure do not vary. In simulation -2- the stabilization is reached soon after $T = 200(\overline{\theta}_{\sigma} = \overline{\theta}_{\varphi} = 2.77, \overline{\alpha}_{\sigma} = 0.66, \overline{\beta}_{\sigma} = 1.41)$, so that the parameter levels and patterns shown in the figure are nearly the steady-state ones. In simulation -3- the black rhomboid vanishes by $T = 220$, and only the small black θ-clusters shown in the figure at $T = 200$ survive in simulations up to $T = 400(\overline{\theta}_{\sigma} = 0.047 \simeq \overline{\theta}_{\varphi} = 0.043, \overline{\alpha}_{\sigma} = 0.16, \overline{\beta}_{\sigma} = 0.07)$. Somehow in the same vein, only the small blank areas in simulation -4- survive at $T = 400(\overline{\theta}_{\sigma} = \overline{\theta}_{\varphi} = 3.10, \overline{\alpha}_{\sigma} = 0.66, \overline{\beta}_{\sigma} = 1.55)$.

Again, as in the fair context, the initial configuration does matter, and the details of the dynamics vary from one simulation to another. Albeit now the ordering $\overline{p}_{\sigma} > \overline{p}_{\varphi}$ keeps regardless the initial configuration, due to the bias inherent to the unfair scenario treated in Fig. 3.

In this unfair context, assuming the average moves $\theta_A = \theta_B = \pi/2, \alpha_A = \beta_A = \pi/4$, it is:

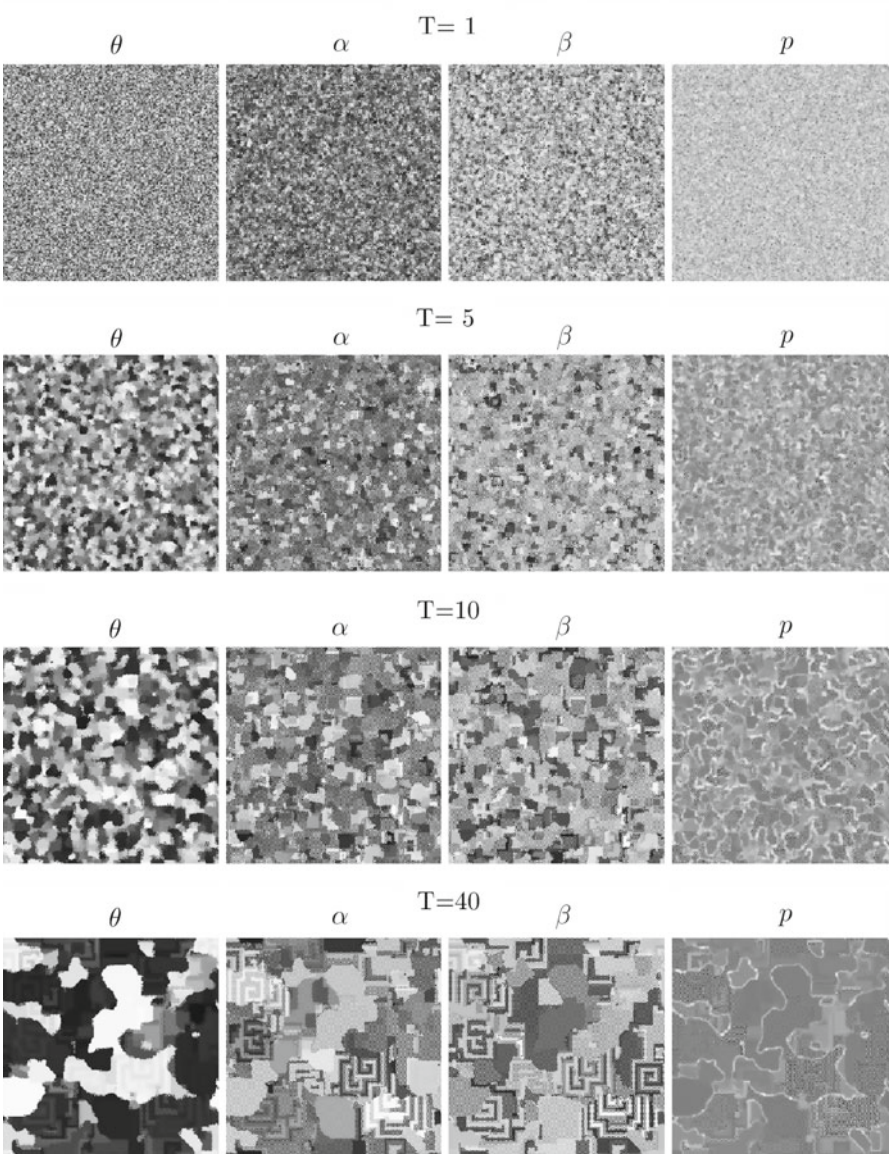

Fig. 2 Initial patterns in the simulation -3- of Fig. 1

$$\hat{U}_A = \frac{1}{\sqrt{2}}\frac{1}{\sqrt{2}}\begin{pmatrix} 1+i & 1+i \\ -(1-i) & 1-i \end{pmatrix}, \hat{U}_B = \frac{1}{\sqrt{2}}\begin{pmatrix} 1 & 1 \\ -1 & 1 \end{pmatrix},$$

$$(\hat{U}_A \otimes \hat{U}_B) = \frac{1}{2}\frac{1}{\sqrt{2}}\begin{pmatrix} 1+i & 1+i & 1+i & 1+i \\ -(1+i) & 1+i & -(1+i) & 1+i \\ -(1-i) & -(1-i) & 1-i & 1-i \\ 1-i & -(1-i) & -(1-i) & 1-i \end{pmatrix}$$

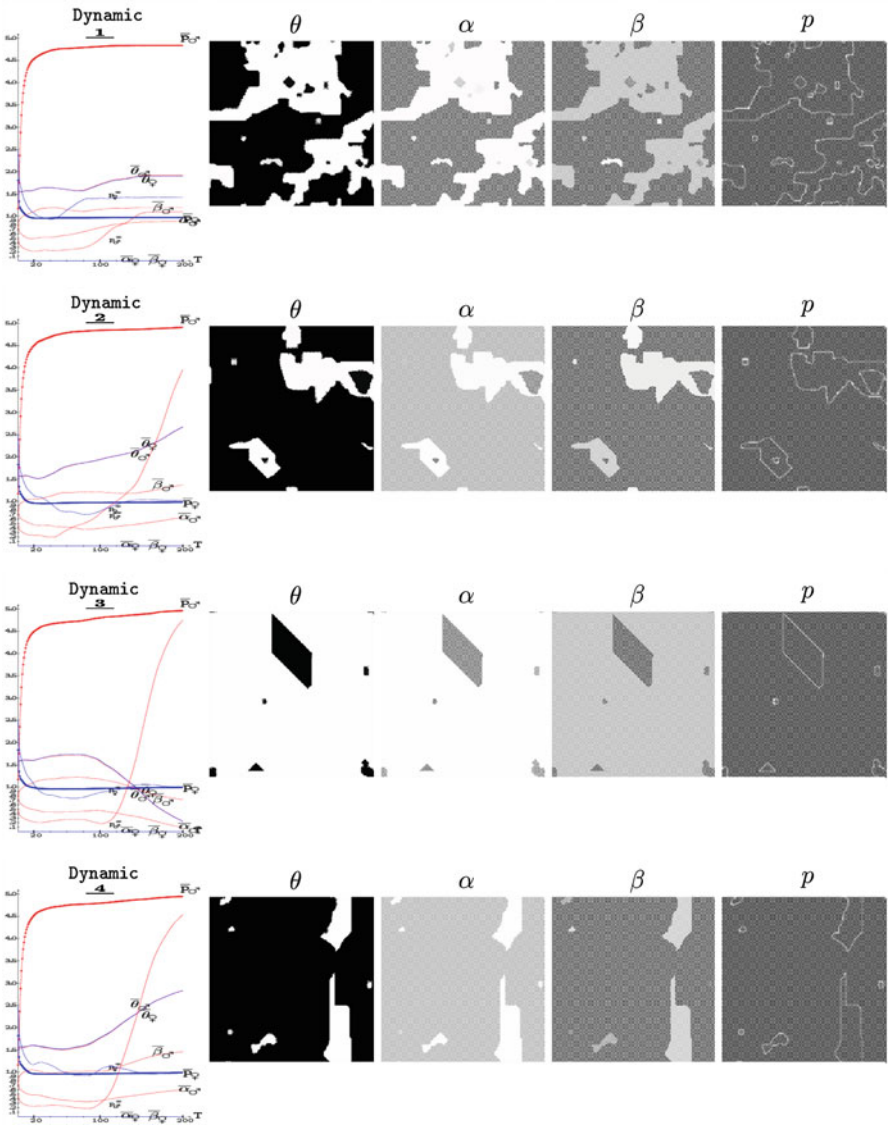

Fig. 3 Simulations of a quantum (5,1)-BOS cellular automaton, where the female players are restricted to classical strategies

$$|\psi_f\rangle = \quad \hat{J}^\dagger(\hat{U}_A \otimes \hat{U}_B)\hat{J}|00\rangle = \hat{J}^\dagger \frac{1}{4}\begin{pmatrix} 2i \\ -2 \\ 2i \\ 2 \end{pmatrix} = \frac{1}{4\sqrt{2}}\begin{pmatrix} 0 \\ -4 \\ 0 \\ 4i \end{pmatrix},$$

$\Rightarrow \mathbf{A} = \begin{pmatrix} 0 & 1/2 \\ 0 & 1/2 \end{pmatrix}$, and, contrary to the expectation (taken into account that B is restricted to classical strategies): $p_B = R/2 > p_A = r/2$.

The two following *partially* unfair scenarios make apparent the unbalanced role played by the α and β parameters, as already pointed out in Sect. 2.

Figure 4 shows four simulations of a quantum (5,1)-BOS cellular automaton, where the female players are not allowed to implement the β parameter. Despite the unfair scenario, the male players are not winning the game such as in the scenario of Fig. 3. In contrast, both kinds of players get in the long-term close mean payoffs as in the fair scenario, with the female type achieving superior payoffs in the four simulations of the figure. It seems that the β parameter does not play a key role with respect to the bias of the proposed quantum scheme, which appears induced by the α parameter. This finding applies even to a greater extent when considering the theoretical payoffs, that are dramatically unbalanced, very high (near 5.0) $p^*_{\female}$, accompanied by very low (near 1.0) $p^*_{\male}$.

In the $\beta_B = 0$ unfair context, assuming the average moves $\theta_A = \theta_B = \pi/2, \alpha_A = \alpha_B = \beta_A = \pi/4$, it is: $\mathbf{A} = \begin{pmatrix} \frac{1}{8} & \frac{1}{2}(\frac{1}{2} + \frac{1}{\sqrt{2}})^2 \\ \frac{1}{2}(\frac{1}{2} - \frac{1}{\sqrt{2}})^2 & \frac{1}{8} \end{pmatrix}$. Thus, $a_{11} > a_{22} \Rightarrow p_{\male} > p_{\female}$.

Figure 5 shows four simulations of a quantum (5,1)-BOS cellular automaton, where the female players are not allowed to implement the α parameter, but are allowed to implement the β parameter. In contrast to what happens in the *fully* unfair scenario of Fig. 3, when impeding to implement the α parameter to the female type players, the payoff of the male type is higher than that of the female type in the four simulations of Fig. 5. But both kinds of payoffs are relatively close, not as happens when impeding both α and β to the female type as in Fig. 3. So to say, this unfair scheme becomes biased towards the male type, so that (1) high mean θ parameter values emerge for both types of players all across the lattice, which blackens the θ-patterns shown in Fig. 5, and (2) the theoretical payoffs are dramatically unbalanced, very high (near 5.0) $p^*_{\male}$, accompanied by very low (near 1.0) $p^*_{\female}$.

In the $\alpha_B = 0$ unfair context, assuming the average moves $\theta_A = \theta_B = \pi/2, \alpha_A = \beta_A = \beta_A = \pi/4$, it is: $\mathbf{A} = \begin{pmatrix} \frac{1}{2}(\frac{1}{2} - \frac{1}{\sqrt{2}})^2 & \frac{1}{2}(\frac{1}{2} + \frac{1}{\sqrt{2}})^2 \\ \frac{1}{8} & \frac{1}{8} \end{pmatrix}$. Thus, $a_{11} < a_{22} \Rightarrow p_{\male} < p_{\female}$.

5 Partial entangling

Adopting an entanglement factor γ, it is:

$$\hat{J} = exp\left(i\frac{\gamma}{2}\hat{D}^{\otimes 2}\right) = \cos(\gamma/2)\hat{I}^{\otimes 2} + i\sin(\gamma/2)\hat{D}^{\otimes 2}, \quad \gamma \in [0, \pi/2].$$

Thus, $\hat{J}^\dagger = \cos(\gamma/2)\hat{I}^{\otimes 2} - i\sin(\gamma/2)\hat{D}^{\otimes 2}$, and

$$\hat{J}|00\rangle = \begin{pmatrix} \cos(\gamma/2) & 0 & 0 & i\sin(\gamma/2) \\ 0 & \cos(\gamma/2) & -i\sin(\gamma/2) & 0 \\ 0 & -i\sin(\gamma/2) & \cos(\gamma/2) & 0 \\ i\sin(\gamma/2) & 0 & 0 & \cos(\gamma/2) \end{pmatrix} \begin{pmatrix} 1 \\ 0 \\ 0 \\ 0 \end{pmatrix} = \begin{pmatrix} \cos(\gamma/2) \\ 0 \\ 0 \\ i\sin(\gamma/2) \end{pmatrix}.$$

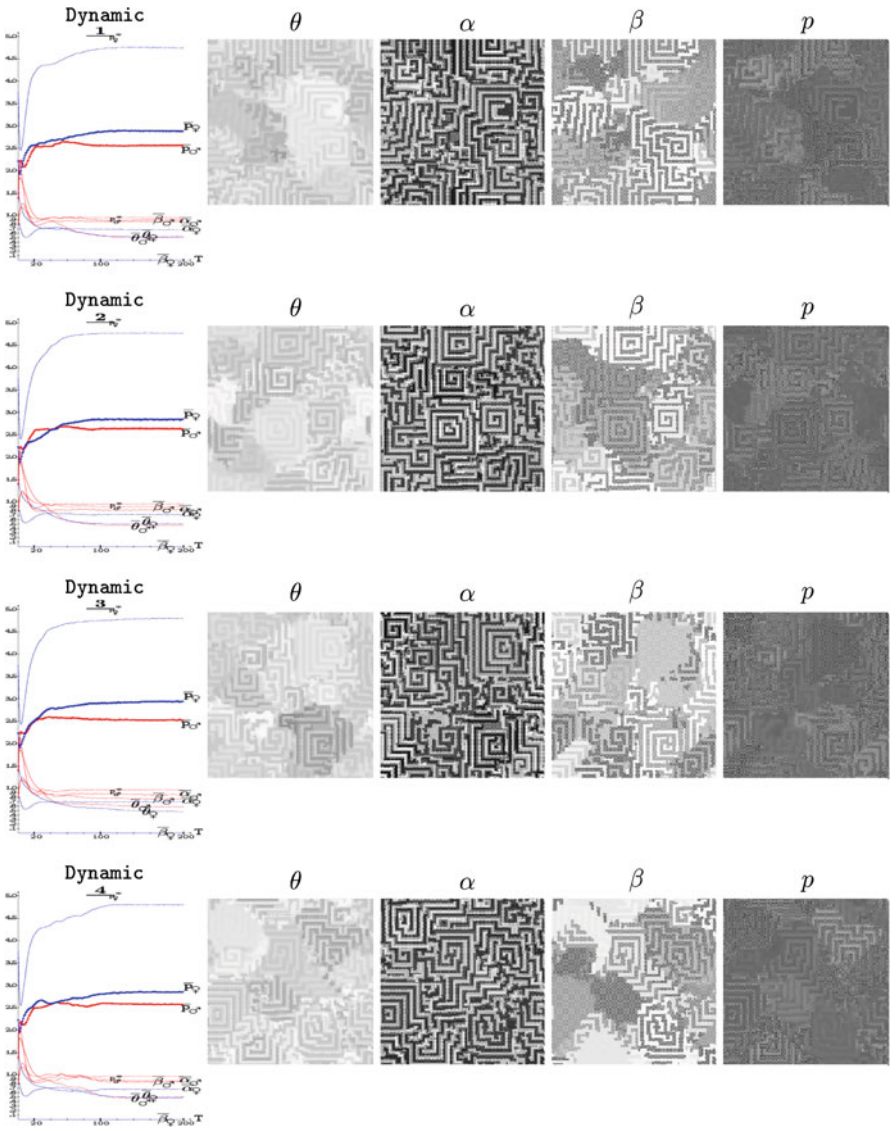

Fig. 4 Simulations of a quantum (5,1)-BOS cellular automaton, where the female players are not allowed to implement the β parameter

Maximal entangling is achieved with $\gamma = \pi/2$, whereas $\gamma = 0$ would refer to the classical uncorrelated context. In the two-parameter model, if $\gamma > \pi/4$, the B player will out score the male player [9,10,12,13].

But in the three-parameter scenario the status of both players varies very much. Thus, for example, with equal middle-level election of the parameters by both players, i.e. $\theta_A = \theta_B = \pi/2$, $\alpha_A = \alpha_B = \beta_A = \beta_B = \pi/4$, it is:

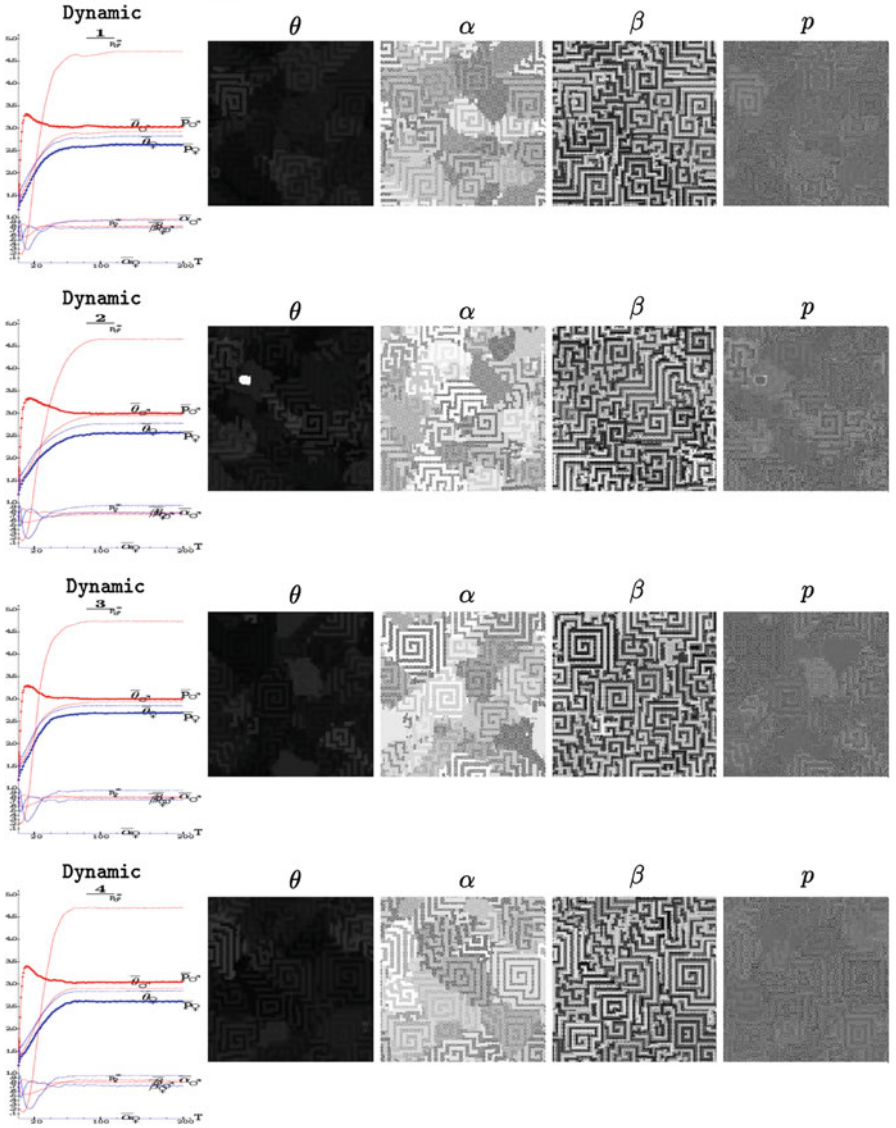

Fig. 5 Simulations of a quantum (5,1)-BOS cellular automaton, where the female players are not allowed to implement the α parameter

$$(\hat{U}_A \otimes \hat{U}_B)\hat{J}|00\rangle = \frac{1}{2}\begin{pmatrix} i & i & i & i \\ -1 & 1 & -1 & 1 \\ -1 & -1 & 1 & 1 \\ -i & i & i & -i \end{pmatrix}\begin{pmatrix} \cos(\gamma/2) \\ 0 \\ 0 \\ i\sin(\gamma/2) \end{pmatrix} = \frac{1}{2}\begin{pmatrix} i\cos(\gamma/2) - \sin(\gamma/2) \\ -\cos(\gamma/2) + i\sin(\gamma/2) \\ -\cos(\gamma/2) + i\sin(\gamma/2) \\ -i\cos(\gamma/2) + \sin(\gamma/2) \end{pmatrix},$$

$$|\psi_f\rangle = \frac{1}{2}\begin{pmatrix} \cos(\gamma/2) & 0 & 0 & -i\sin(\gamma/2) \\ 0 & \cos(\gamma/2) & i\sin(\gamma/2) & 0 \\ 0 & i\sin(\gamma/2) & \cos(\gamma/2) & 0 \\ -i\sin(\gamma/2) & 0 & 0 & \cos(\gamma/2) \end{pmatrix}\begin{pmatrix} i\cos(\gamma/2) - \sin(\gamma/2) \\ -\cos(\gamma/2) + i\sin(\gamma/2) \\ -\cos(\gamma/2) + i\sin(\gamma/2) \\ -i\cos(\gamma/2) + \sin(\gamma/2) \end{pmatrix}$$

$= \frac{1}{2}\begin{pmatrix} -\sin\gamma + i\cos\gamma \\ -1 \\ -1 \\ \sin\gamma - i\cos\gamma \end{pmatrix}$. Again, we have: $\mathbf{A} = \begin{pmatrix} 1/4 & 1/4 \\ 1/4 & 1/4 \end{pmatrix}$, and consequently, $p_{\female} = p_{\male} = \frac{R+r}{4}, \forall\gamma$.

Four simulations of the quantum (5,1)-BOS cellular automaton with $\gamma = \pi/4$ are shown in Fig. 6. As expected from the just above derivation of the mean payoffs in the equal middle level election of the parameters, the initial actual mean payoffs in these simulations are (again) close to $(R + r)/4 = 6/4 = 1.5$.

In two of these simulations in Fig. 6 the male type of players outperforms the female, whereas the contrary happens in the other two simulations. In contrast to what happens in the fully entangled simulation of Fig. 1, in Fig. 6 the theoretical payoffs (p^*) evolve under the actual mean payoffs, and do not *diverge* to the extent they do Fig. 1. Figures 1 and 6 share the not dramatic deviation during the simulations of the mean α and β parameter values of both kinds of players from the initial $\pi/4 = 0.78$, which is perhaps even smaller in the case of Fig. 6. Maze-like structures predominate for both α and β parameters of Fig. 6, whereas nucleation predominates in what respect the θ parameter, much as in the fully entangled case of Fig. 1.

Short initial transition periods are observed in the simulations in Fig. 6, but the mean payoffs evolve in a not so parallel way and their stability appears to be not as strong as in Fig. 1. Thus, in simulations -1- and -3-, the mean payoffs soon stabilize after $T = 200$, but in simulations -2- and -4- the mean payoffs apparently diverge. The mean payoffs of simulation -4- slowly diverge, due to a slow increase of the θ values, up to $T = 1000$, when the dynamics achieve an almost-steady configuration with: $p_{\female} = 3.09$, $p_{\male} = 2.62$. In contrast an almost-steady configuration is achieved in simulation -2- after a notable decrease in the θ values, with: $p_{\female} = 2.54$, $p_{\male} = 3.16$), at $T = 500$.

Further decreasing of the entangling parameter γ would diminish the *quantum*, i.e., *entangled*, component of the model (2). In the limit case, $\gamma = 0$, it is $\hat{J}^\dagger = \hat{J} = I$, so that the classical formulation is recovered with:

$$|\psi_f\rangle = \begin{pmatrix} e^{i\alpha_A}\cos\omega_A e^{i\alpha_B}\omega_B \\ -e^{i\alpha_A}\cos\omega_A e^{-i\beta_B}\sin\omega_B \\ -e^{-i\beta_A}\sin\omega_A e^{i\alpha_B}\cos\omega_B \\ e^{i\beta_A}\sin\omega_A e^{-i\beta_B}\sin\omega_B \end{pmatrix} \rightarrow \mathbf{A} = \begin{pmatrix} \cos^2\omega_A \\ \sin^2\omega_A \end{pmatrix}\begin{pmatrix} \cos^2\omega_A & \sin^2\omega_B \end{pmatrix}.$$

In spatial simulations with $\gamma = \pi/8$, the θ patterns become highly black-black defined (with no *maze* incrustations), but the α and β patterns still retain their characteristic *maze* aspect. But if $\gamma = 0$, the α and β patterns lose their *maze* aspect and somehow present the *patchwork* aspect of the θ parameter. The classical scenario has been properly studied, i.e., without the α and β parameters, in [2].

6 Conclusions and future work

The quantum CA formulation of the spatial battle of the sexes evolves in a notably distinct manner when considering the full space of feasible strategies, which enables three

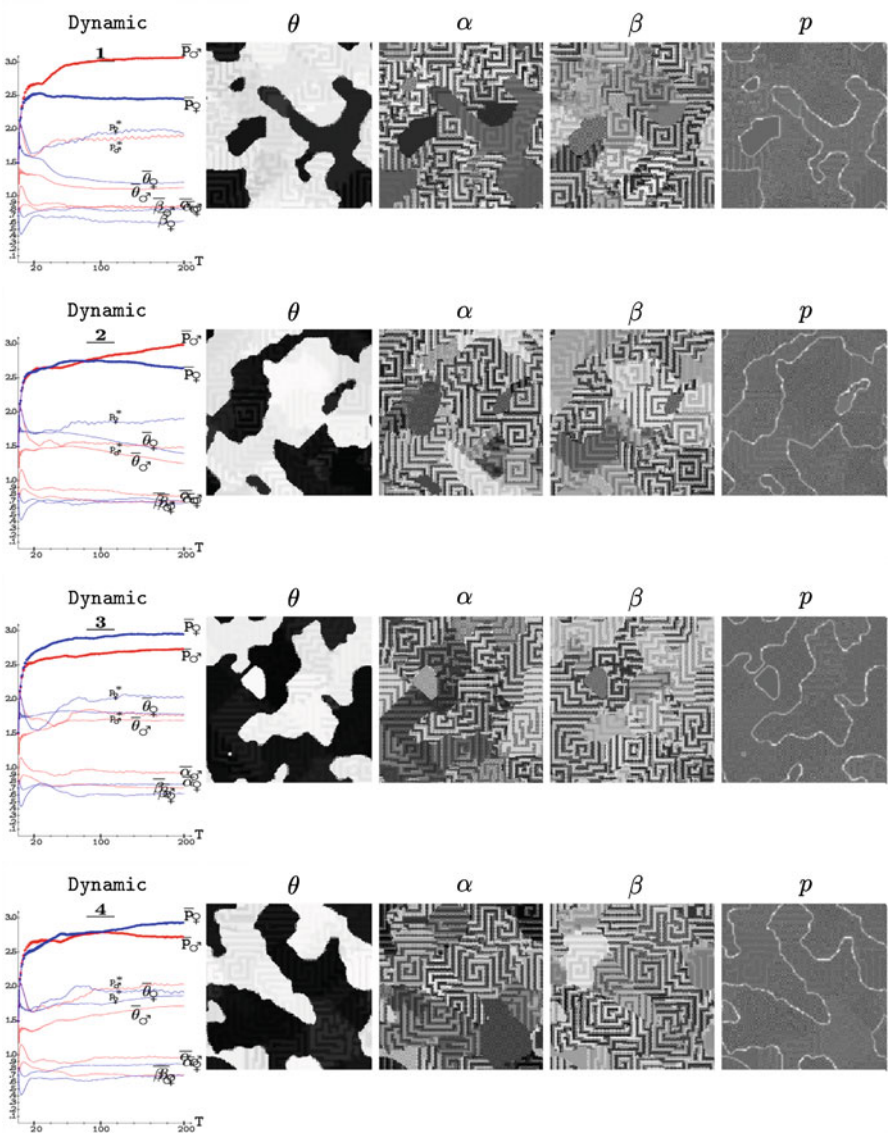

Fig. 6 Simulations of a three-parameter quantum (5,1)-BOS cellular automaton with $\gamma = \pi/4$. *Left* evolving mean parameters and payoffs. *Center* parameter patterns at $T = 200$. *Right* payoff patterns at $T = 200$

tuning parameters (3P), compared to the evolving dynamic emerging when restraining the strategies to a subset with only two parameters (2P) previously studied [1]. The most distinctive trait is that of the balanced expectations of both kinds of players in the 3P scenario compared to the bias towards the female player in the 2P formulation. The spatial structure enables self-organization phenomena which produce very high mean payoffs. Allowing three parameters in the strategies supports similar mean payoffs for both kinds of players.

Other quantization schemes [15,19,20] deserve particular studies in the spatial context. In particular the scheme introduced by Marinatto and Weber [18], in which the initial state of the game $|\psi_i\rangle$ is a linear combination of the vectors of the base $(|00\rangle, |01\rangle, |10\rangle, |11\rangle)$, and differs from the earlier proposed of Eisert et al. [11] by the absence of the reverse gate $J^\dagger$. The study of the features of the emerging patterns [8] is due in all these contexts.

As long as only the results from the last round are taken into account and the outcomes of previous rounds are neglected, the model considered here may be termed *ahistoric* or, better, Markovian. We plan to deal with models with (proper) memory in the near future. We will adopt a simple approach to memory implementation: the general imitation of the best rule will remain unaltered, but it will operate on the trait payoffs and parameters of every player, constructed from the previous rounds. We have studied the effect of this kind of embedded memory in the classical spatial BOS in [3,4]. Technically, its extension to the quantum context will demand the additional effort of dealing with three parameters (θ, α, β) instead of one (θ or the F-probability).

Further study is due on structurally dynamic quantum games, in games with asynchronous and probabilistic updating, as well as on the effect of increasing degrees of spatial dismantling. These are deviations from the canonical cellular automata paradigm which may lead to more realistic models. Particularly, with embedded tuneable memory [5].

Last but not least, other games, particularly the prisoner's dilemma, will be taken into account in the near future.

Acknowledgments This work was supported by the Spanish grant no. MTM2012-39101-C02-01.

References

1. Alonso-Sanz, R.: A quantum battle of the sexes cellular automaton. Proc. R. Soc. A **468**, 3370–3383 (2012)
2. Alonso-Sanz, R.: The spatialized, continuous-valued battle of the sexes. Dyn. Games Appl. **22**, 2,2,177–194 (2012)
3. Alonso-Sanz, R.: Self-organization in the battle of the sexes. Int. J. Mod. Phys. C **22**(1), 1–11 (2011)
4. Alonso-Sanz, R.: Self-organization in the spatial battle of the sexes with probabilistic updating. Phys. A **390**, 2956–2967 (2011)
5. Alonso-Sanz, R.: Dynamical Systems with Memory. World Scientific, Singapore (2011)
6. Benjamin, S.C., Hayden, P.M.: Comment on "Quantum games and quantum strategies". Phys. Rev. Lett. **87**(6), 069801 (2001)
7. Binmore, K.: Fun and Games. D.C. Heath, Lexington (1992)
8. Dieckmann, U., Law, R., Metz, J.A.J.: The Geometry of Ecological Interactions. Simplifying Spatial Complexity. Cambridge University Press, IIASA, Cambridge (2000)
9. Du, J.F., Xu, X.D., Li, H., Zhou, X., Han, R. et al.: Entanglement playing a dominating role in quantum games. Phys. Lett. A **89**(1–2), 9–15 (2001)
10. Du, J.F., Li, H., Xu, X.D., Zhou, X., Han, R.: Phase-transition-like behaviour of quantum games. J. Phys. A Math. Gen. **36**(23), 6551–6562 (2003)
11. Eisert, J., Wilkens, M., Lewenstein, M.: Quantum games and quantum strategies. Phys. Rev. Lett. **83**(15), 3077–3080 (1999)
12. Flitney, A.P., Abbott, D.: An introduction to quantum game theory. Fluctuation Noise Lett. **2**(4), R175–R187 (2002)
13. Flitney, A.P., Abbott, D.: Advantage of a quantum player over a classical one in 2 × 2 quantum games. Proc. R. Soc. Lond. A **459**(2038), 2463–2474 (2003)

14. Flitney, A.P., Hollengerg, L.C.L.: Nash equilibria in quantum games with generalized two-parameter strategies. Phys. Lett. A **363**, 381–388 (2007)
15. Frąckiewicz, P.: The ultimate solution to the quantum battle of the sexes game. J. Phys. A Math. Theor. **42**(36), 365305 (2009)
16. Harsanyi, J., Selten, R.: A General Theory of Equilibrium Selection in Games. The MIT Press, Cambridge (1988)
17. Hofbauer, J., Sigmund, K.: Evolutionary Games and Population Dynamics. Cambridge University Press, Cambridge (2003)
18. Marinatto, L., Weber, T.: A quantum approach to static games of complete information. Phys. Lett. A **272**, 291–303 (2000)
19. Nawaz, A.,Toor, A.H.: Dilemma and quantum battle of sexes. J. Phys. A Math. Gen. **446**, 37,15,4437–4443 (2004)
20. Nawaz, A., Toor, A.H.: Generalized quantization scheme for two-person non-zero sum games. J. Phys. A Math. Gen. **42**(36), 365305 (2004)
21. Owen, G.: Game Theory. Academic Press, London (1995)
22. Schiff, J.L.: Cellular Automata: A Discrete View of the World. Wiley, London (2008)
23. Wiesner, K.: Quantum Cellular automata. http://arxiv.org/abs/0808.0679 (2009)